Published in final edited form as:
Biomaterials. 2011 August ; 32(24): 5568–5580. doi:10.1016/j.biomaterials.2011.04.038.

The Stimulation of the Cardiac Differentiation of Mesenchymal Stem Cells in Tissue Constructs that Mimic Myocardium Structure and Biomechanics

Jianjun Guan[1], **Feng Wang**[1], **Zhenqing Li**[1], **Joseph Chen**[2], **Xiaolei Guo**[1], **Jun Liao**[2], and **Nicanor I. Moldovan**[3]

[1]Department of Materials Science & Engineering, The Ohio State University, Columbus, OH, 43210

[2]Department of Agricultural & Biological Engineering, Mississippi State University, Mississippi State, MS, 39762

[3]Davis Heart and Lung Research Institute, The Ohio State University, Columbus, OH, 43210

Abstract

We investigated whether tissue constructs resembling structural and mechanical properties of the myocardium would induce mesenchymal stem cells (MSCs) to differentiate into a cardiac lineage, and whether further mimicking the 3-D cell alignment of myocardium would enhance cardiac differentiation. The tissue constructs were generated by integrating MSCs with elastic polyurethane nanofibers in an electrical field. Control of processing parameters resulted in tissue constructs recapitulating the fibrous and anisotropic structure, and typical stress-strain response of native porcine myocardium. MSCs proliferated in the tissue constructs when cultured dynamically, but retained a round morphology. mRNA expression demonstrated that cardiac differentiation was significantly stimulated. Enhanced cardiac differentiation was achieved by 3-D alignment of MSCs within the tissue constructs. Cell alignment was attained by statically stretching tissue constructs during culture. Increasing stretching strain from 25% to 75% increased the degree of 3-D cell alignment. Real time RT-PCR results showed that when cells assuming a high degree of alignment (with application of 75% strain), their expression of cardiac markers (GATA4, Nkx2.5 and MEF2C) remarkably increased. The differentiated cells also developed calcium channels, which are required to have electrophysiological properties. This report to some extent explains the outcome of many in vivo studies, where only a limited amount of the injected MSCs differentiated into cardiomyocytes. It is possible that the strain of the heartbeat (∼20%) cannot allow the MSCs to have an alignment high enough for a remarkable cardiac differentiation. This work suggests that pre-differentiation of MSCs into cardiomyocytes prior to injection may

Corresponding Author: Jianjun Guan, Ph.D. Assistant Professor, Department of Materials Science and Engineering, The Ohio State University, 2041 College Road, Columbus, OH 43210, Phone: 614-292-9743, guan.21@osu.edu.

result in a greater degree of cardiac regeneration than simply injecting un-differentiated MSCs into heart.

Keywords

electrospinning; tissue-specific constructs; mesenchymal stem cell; myocardium

1. Introduction

Myocardial infarction (MI) causes a loss of heart muscle and a decrease of heart function. Various therapeutic strategies have been used to treat MI [1]. However, normal heart function after MI cannot be restored because adult cardiomyocytes are less regenerative and endogenous cells are unable to produce sufficient cardiomyocytes for effective regeneration. Cardiac stem cell therapy is considered to be a promising approach for cardiac regeneration and heart function restoration [2,3]. It delivers stem cells into the infarcted heart where they differentiate into cardiomyocytes. The regenerated heart muscle then integrates with the surrounding heart muscle and functions synchronically.

Various types of stem cells have cardiac differentiation potential, including mesenchymal stem cells (MSCs) [4-9], embryonic stem cells (ESCs) [10], induced pluripotent stem cells (iPSCs) [11], and cardiac progenitor cells [12-14]. Among these cell types, MSCs have been widely used for cardiac cell therapy because they can not only differentiate into cardiomyocytes but also secrete growth factors that may improve angiogenesis [4-9]. Cardiac differentiation of MSCs can be achieved in vivo and in vitro. In vivo studies using various animal models have demonstrated that some MSCs differentiate into cardiomyocytes after injection into hearts [4-9]. Recent clinical trials also showed that MSCs significantly improved cardiac function [15-17]. The in vitro cardiac differentiation is accomplished by either using biochemicals such as 5-azacytidine (5-aza) [18-20] or co-culturing with cardiomyocytes [21,22].

To deliver stem cells into hearts, a tissue engineering approach has been used. This involves the engineering of stem cell-populated tissue constructs that are subsequently patched onto the infarcted heart surface. Successful myocardium regeneration and heart function improvement are largely dependent on the properties of scaffolds [23-25]. Biomimetic scaffolds that mimic advantageous features of the extracellular matrix (ECM) in myocardium are believed to facilitate tissue development, as they provide a native-like template that allows cells to organize into the tissue specific structure [24,25]. However, the effectiveness of the stem cells for cardiac therapy depends on their cardiac differentiation. Thus, the ideal tissue constructs should stimulate stem cell differentiation into a cardiac lineage. Current cardiac tissue constructs are mostly microporous scaffolds and hydrogels based on natural polymers such as collagen [24-27] and polysaccharide [22,28,29], and synthetic polymers such as polyurethane [30,31] and poly(glycerol-sebacic acid) [23,24]. These scaffolds and hydrogels differ from the native myocardium, either structurally or mechanically, and are unable to produce a native-like microenvironment for stem cell differentiation and function [32]. Studies based on these scaffolds have demonstrated that MSCs cannot readily differentiate into a cardiac lineage without using biochemicals such as

5-aza [22,29]. In this study we hypothesized that tissue constructs that mimic the structural and mechanical properties of the myocardium, may provide a native-like microenvironment for stimulating stem cell differentiation into a cardiac lineage. We also hypothesized that mimicking 3-D cell alignment in the myocardium would further enhance cardiac differentiation in these tissue constructs.

The objective of this work was to generate tissue constructs mimicking structural and mechanical properties of the myocardium, achieve 3-D cell alignment in the tissue constructs, and examine if MSCs would differentiate into a cardiac lineage in the tissue constructs. The tissue constructs were fabricated by concurrently electrospraying cells and electrospinning elastic fibers. This allowed the fast generation of cellularized tissue constructs for the study of stem cell behavior at the 3-D level. Electrospinning technique was used to create fibers that mimic diameter and alignment of the collagen fibers in the myocardium. The mechanical properties of the tissue constructs were manipulated in terms of fiber polymer type, fiber alignment and cell density. In order to achieve 3-D cell alignment, tissue constructs were stretched statically during the culture.

The relation between stretching strain and degree of cell alignment was investigated. MSC differentiation in the tissue constructs was quantified by the expression of cardiac markers and development of ion channels.

2. Materials and Methods

2.1 Materials

Pluronic L31 (EO_2-PO_{16}-EO_2, MW ~1100, BASF) and trimethylcarbonate (TMC, Boehringer Ingelheim) were vacuum dried overnight prior to use. Butanediisocyanate (BDI, Fluka) and putrescine (Aldrich) were vacuum distilled before synthesis. Stannous octoate (Sigma) and dimethyl sulfoxide (DMSO) were dried over 4 Å molecular sieves. Gelatin (type A, Acros) and 1,1,1,3,3,3-hexafluoro-2-propanol (HFIP, Oakwood Products) were used as received.

2.2. Polymer Synthesis

Block copolymer diol PTMC-PEO-PPO-PEO-PTMC was synthesized through ring-opening polymerization of TMC by using PEO-PPO-PEO as an initiator and stannous octoate as a catalyst (Figure 1) [33-35]. The molar ratio of TMC/PEO-PPO-PEO was 4. The polymerization was conducted at 110°C for 18 h under a nitrogen atmosphere. The yielded copolymer was purified with ethyl ether and hexane, then dried in a vacuum oven at 50°C for 24 h.

The poly(ester carbonate urethane)urea (PECUU) based on the PTMC-PEO-PPO-PEO-PTMC diol was synthesized by a two-step solution polymerization (Figure 1) [33,34]. In brief, the synthesis was conducted in a 250 mL three-necked flask equipped with a nitrogen inlet and outlet. A 1 wt% BDI (7.98 mmol) solution in DMSO was added into the flask followed by a 10 wt% copolymer diol (3.99 mmol) solution in DMSO. Two drops of stannous octoate was then added. The reaction was carried out at 80°C for 3.5 h under continuously stirring. The solution was then cooled to room temperature, and a 1 wt%

putrescine solution (3.99 mmol) was subsequently added. The reaction was continued for 12 h at room temperature. The polymer solution was precipitated in the saturated potassium chloride solution. The polymer was then immersed in de-ionized water for 24 h to leach out the salt, and finally dried under vacuum at 50°C for 24 h.

2.3. MSC electrospraying and characterization

MSCs were electrosprayed under high voltage (28 kV) to investigate the effect of electrical treatment on MSC survival, growth, morphology and multipotency. Human MSCs (Lonza) were cultured in T-175 flasks using culture medium containing Dulbecco's modified Eagle's medium (DMEM) and 10% FBS [36]. The cells at passage 10 were used. Previous work demonstrated that MSCs at this passage preserved phenotype and multipotentcy [36-38]. MSCs were suspended in the culture medium containing 2% gelatin A to reach a density of 1 million/mL. The MSC suspension was electrosprayed from a sterile stainless-steel capillary (I.D. 0.047″, charged with +18 kV) into a T-25 flask that was placed on an aluminum plate charged with -10 kV. The electrosprayed MSCs were divided into three parts for 1) staining with Trypan Blue to investigate if electrical treatment under high voltage causes cell death [39]; 2) seeding in a 96-well culture plate to determine growth rate and gene expression of the as-electrosprayed cells; and 3) seeding into a flask to expand cells for evaluating if electrospraying affects longer-term cell growth and multipotency. MSCs followed the same treatment process but without applying an electrical field, were used as the control.

To characterize growth of as-electrosprayed cells seeded in a 96-well plate, an MTT assay was used after 1, 3 and 5 days of culture [38]. The gene expression was characterized by RT-PCR. Total RNA was extracted by TRIzol according to the manufacture's instruction. Approximately 1μg RNA was used to synthesize cDNA by High Capacity cDNA Reverse Transcription Kits. PCR was performed with a Mastercycler ep gradient S thermal cycler and Platinum *Taq* DNA Polymerase. Primers used are listed in Table 1. The conditions for PCR were 94°C for 2 min, 40 cycles (94°C for 1 min, 58°C for 1 min and 72°C for 2 min) and a final 72°C extension for 10 min [40]. The amplified product was then analyzed by electrophoresis in 2% agarose gel.

The electrosprayed cells that were seeded in the flask were expanded twice and then subjected to cell growth and differentiation characterization. The cell growth was assessed by seeding cells in a 96-well plate followed by MTT assay after 1, 3 and 5 days of culture [38]. As the MSCs are multipotent and capable of differentiating into osteogenic, chondrogenic and adipogenic lineages, the electrosprayed cells were induced to differentiate into these lineages to investigate if electrical treatment affects multipotency. To induce osteogenesis, cells were cultured in an osteogenic growth medium (10 nM dexamethasone (DEX), 5 mM glycerophosphate, 50 mg/ml ascorbic acid (AA), and 10 nM 1,25-dihydroxy vitamin D3). On day 21, cells were stained for alkaline phosphatase (ALP) activity [37,41]. To induce chondrogenesis, cells were seeded in a high density (2.5×10^5 cells/mL) and allowed to grow for 21 days in a serum-free medium (DMEM, ITS Premix, 50 mg/ml AA, 40 mg/ml L-proline, 100 mg/ml sodium pyruvate, 0.1 M DEX, and 10 ng/ml recombinant human transforming growth factor TGF-β1). On day 21, alcian blue staining was performed

to detect sulfated glycosaminoglycan (sGAG) [37,41]. For induction of adipogenic differentiation, MSCs were cultured for 21 days in an adipogenic medium containing DMEM with 10% FBS, and supplemented with 0.5 mmol/L 3-isobutyl-1-methylxanthine (IBMX), 1 μg/ml insulin, and 1 μmol/L dexamethasone. Cell differentiation was evaluated by accumulation of intracellular neutral lipids stained with Oil Red O [37,41].

2.4. Tissue construct fabrication

MSC-populated tissue constructs were fabricated by simultaneously electrospinning PECUU nanofibers and electrospraying MSCs, using an approach modified from our previous reports [38,42]. In brief, 15 wt% PECUU in HFIP was fed at 4.5 mL/h into a capillary charged at +15 kV. The tip of the capillary was 15 cm away from the collecting mandrel (diameter 11 cm). MSCs labeled with live cell marker CellTracker Green CMFDA (5-chloromethylfluorescein diacetate, concentration 10 μM) were suspended in the culture medium containing 2% gelatin A. Two different cell densities 8 and 30 million/mL were used. The cell suspension was fed at 15 mL/h into a sterile capillary that was charged at +10 kV and 5 cm away from the collecting mandrel. Two capillaries were offset at 135° to avoid electrical field interference. The collecting mandrel was charged at -10 kV and rotated at 1500 rpm. The fabrication typically lasted for 40 min, which yielded tissue constructs with a thickness ∼200 μm. For clarity, the tissue constructs fabricated from cell densities 8 and 30 million/mL were abbreviated as 8M and 30M, respectively. After fabrication the tissue constructs were peeled off from the mandrel and immersed in the culture medium to remove any possible residual solvent. The medium was changed twice every 30 min. The fabricated tissue constructs were then cultured in the medium for 24 h.

2.5. Characterization of as-fabricated tissue constructs

The as-fabricated tissue constructs were characterized in terms of cell distribution in the construct, fiber alignment and mechanical properties. The cell distribution was imaged by a Zeiss LM 550 confocal laser scanning microscope (CLSM). Representative images were taken as a series of stacked images. Fiber morphology was characterized by SEM. Before imaging, samples were immersed in phosphate buffered saline (PBS, pH=7.4) for 3 days to completely remove gelatin and cells on the surface. This process allowed better imaging fibers that otherwise cannot be clearly imaged due to the interference of gelatin and cells. The samples were then lypholized, sputter-coated and imaged in a FEI NOVA nanoSEM. Fiber alignment was calculated according to a method described previously [43]. Vertical lines were drawn in a SEM image (at least three images were used), and angles between the fibers and the vertical lines were measured using Image J software. At least 100 angles were measured from each SEM image. The mean angle was calculated and considered as the alignment direction (0°) of the scaffold. The measured angles were then normalized. Histograms of these angles were plotted over a +90° to −90° range in 5° intervals. The degree of alignment was defined as the percentage of fibers within ±20° of the alignment direction.

Tissue construct mechanical properties were measured by biaxial tensile testing. The biaxial testing is considered to be much more physiologically relevant especially for soft tissues like myocardium that exhibits complex, mechanically anisotropic behaviors [44]. To test biaxial

mechanical properties, samples were cut into size of 12 mm × 12 mm, with one edge aligned along the fiber-preferred direction (PD) and another edge aligned with cross-fiber direction (XD). The biaxial mechanical properties of porcine hearts were also tested to compare their mechanical properties with those of the tissue constructs. Fresh porcine hearts were obtained from a local slaughterhouse and transported to the laboratory in chilled PBS. Similarly, a 12 mm × 12 mm × 2 mm square specimen was trimmed from the fresh hearts with edges along PD and XD directions of the specimen. Three specimens were tested for each group.

A detailed description of the biaxial device and testing protocol was reported in references [45,46]. In brief, four fiducial markers were placed in the center of the specimen to track the deformation. A total of 8 loops of 000 polyester suture of equal length were attached to the sample via stainless steel hooks, with two loops on each side. The tests were implemented with the samples completely immersed in PBS at room temperature. Membrane tension (force/unit length) was applied along each axis and was ramped slowly from a pre-stress, ∼0.5 N/m, to a peak value that depended upon the protocol by using a triangular waveform. Specimens were first preconditioned for 10 contiguous cycles and then loaded up to 30:30 N/m equibiaxial tension. Due to possible tissue tear at the hook sites at higher tension level, porcine myocardium specimens were only loaded up to 30 N/m, which corresponds to a stress level of 10 kPa. Biaxial behavior of tissue constructs and native myocardium was correspondingly compared in a stress range from 0 to 10 kPa. Net extensibility was characterized by an areal strain under 10 kPa stress, $(\lambda_{PD} \cdot \lambda_{XD} - 1) \times 100\%$, where λ_{PD} and λ_{XD} were the maximum stretches along PD and XD directions, respectively. Hysteresis, a parameter that reflects energy dissipation, was measured by normalizing the enclosed area of loading and unloading curves (stress vs. strain) to the area underneath the loading curve [45,46].

2.6. Tissue construct culture

After fabrication and culturing in the culture medium for 24 h, the tissue constructs were cut into 5 cm × 2.5 cm pieces. The samples were divided into two groups: one for culture without stretching, the other was stretched to achieve 3-D cell alignment. To culture tissue constructs without stretching, the constructs were placed in spinner flasks and stirred at 20 rpm. Each spinner flask was supplemented with 100 mL of culture medium. To culture tissue constructs under stretching, the constructs were placed in a stretching apparatus, and each received a predefined strain (25%, 50% or 75%). The apparatuses were then placed in the spinner flasks.

2.7. Tissue construct characterization

At defined time points (1, 3 and 7 days), the tissue constructs were taken out for characterization of DNA content, cell morphology, cell alignment, and mRNA expression. To measure DNA content, tissue constructs were digested with papain solution (0.125 mg/mL papain in 100mM sodium phosphate, 10 mM EDTA buffer, 100 mM L-cystein, pH=6.5) at 60°C. The DNA content was quantified with a PicoGreen dsDNA (for live cells) assay [47].

Cell morphology was characterized by CLSM. Samples were rinsed with PBS, fixed with 3.7% paraformaldehyde, permeabilized with 0.1% Triton X-100 and stained with rhodamine phalloidin (Molecular Probes) for F-actin. Representative images were taken as a series of stacked images. Cell alignment in the tissue constructs was characterized by cell anisotropic index. A customized MATLAB program was devised to calculate the cell anisotropic index [24,48]. In general, the CLSM images were first processed by the Welch window method to remove the edge effect. A fast Fourier transformation algorithm was then applied to obtain the power spectrum pattern from the windowed image. An intensity-orientation histogram plot was calculated based on the power spectrum. The anisotropic index was defined as the possibility of cells being aligned within ±20° of the principle aligned axis, normalized to that of a purely random sample. This makes the anisotropic index value for a completely round cell 0. A higher anisotropic index means higher degree of cell alignment.

To analyze mRNA expression of MSCs during the culture, tissue constructs were placed in the TRIzol solution to extract RNA. cDNA was synthesized using High Capacity cDNA Reverse Transcription Kits. Real-time RT-PCR was performed in triplicate for each sample with Maxima SYBR green/fluorescein master mix on an Applied Biosystems 7900 system with an annealing temperature of 55°C. Cardiac markers MEF2C, GATA4 and Nkx2.5 (sequences are listed in Table 1) were assessed. Fold differences were calculated using the standard Δ ΔCt method with β-actin as the housekeeping gene [49].

2.7. Statistics

Results are expressed as the mean ± standard deviation. Two-way ANOVA was employed to evaluate MSC viability (by MTT), DNA content, mechanical properties and cell differentiation. The Neuman-Keuls test was used for post hoc assessments of the differences between samples.

3. Results

3.1. PECUU synthesis

The PECUU was synthesized using a pentablock copolymer PTMC–PEO–PPO–PEO–PTMC as the soft segment, and 1,4-diisocyanatobutane and putrescine as the hard segment. PECUU film was highly flexible and soft, with a tensile strength of 28±4 MPa, breaking strain of 830±80%, and modulus of 5.5±0.9 MPa. The polymer had a weight loss of 5% after incubation in PBS for 6 weeks. The PECUU was cytocompatible. Considering the adherent smooth muscle cell density on the tissue culture plate to be 100%, the cell adhesion on the PECUU was 109%. There was no significant difference between the tissue culture plate and PECUU.

3.2. Effect of electrical treatment on MSC growth and multipotency

Tissue constructs were fabricated by simultaneously electrospinning PECUU fibers and electrospraying MSCs. Prior to tissue construct fabrication, MSCs were electrosprayed under high voltage to evaluate if the electrical treatment affected MSC survival, growth and multipotentcy. After electrospraying under 28 kV, 93±1% of cells remained viable. Figure 2A shows the growth kinetics of MSCs right after and two passages after electrospraying.

The growth kinetics of the electrosprayed MSCs did not show any significant difference from that of the non-electrosprayed MSCs, even two passages after electrospraying. Phase contrast images (not shown) demonstrated that there was no morphological difference between cells with or without electrospraying. These results demonstrated that the electrospraying under high voltage did not change MSC growth and morphology.

Further studies evaluated the influence of electrospraying on MSC multipotency. Figure 2B shows the gene expression of MSCs before and after electrospraying. The mRNA markers corresponding to ostogenesis (COL1A1 and osteonectin) and chondrogenesis (PPARγ2) were evaluated. Similar to MSCs without electrical treatment, the electrosprayed MSCs exhibited all of these markers, demonstrating that the cells remained multipotent after electrical treatment. Multipotency of the electrosprayed MSCs was further confirmed by their differentiation potential. Following the established differentiation protocols used to identify MSC multipotency, the electrosprayed MSCs were induced to differentiate into osteo-, chondro- and adipo-lineages. The differentiation was conducted in osteogenesis, chondrogenesis or adipogenesis growth medium for 21 days, respectively. Successful differentiation was confirmed by Alcian blue staining for sulfated proteoglycan (chondrogenesis, Figure 2C1), alizarin red staining for calcified extracellular matrix (osteogenesis, Figure 2C2), and oil red O staining for lipid droplets (adipogenesis, Figure 2C3). These results demonstrated that the electrical treatment under high voltage retained MSC multipotency.

3.3. Tissue construct fabrication

Tissue constructs were generated by concurrently electrospraying MSCs and electrospinning PECUU fibers. This process sustained rapidly forming cell populated tissue constructs with controlled cell density. After 40 min of fabrication, the obtained tissue constructs typically assumed a thickness of ~200 μm. MSCs were distributed uniformly along the thickness of the tissue constructs, as confirmed by the Z-stack CLSM images of CMFDA-stained, live MSCs (Figure 3A). MSC density in the tissue constructs was controlled by initial MSC density in the cell suspension. dsDNA content (for live cells) was used to characterize MSC density in the construct, which was found to be proportional to the initial MSC density (Figure 6). Increasing initial MSC density from 8 to 30 million/mL increased the dsDNA content from 219.2±27.4 to 755.5±43.3 ng/mg scaffold. The tissue constructs appeared to be highly cellularized when the initial cell density was 8 million/mL (Figure 3A). These results demonstrated that the electrospinning/electrospraying technique is efficient in the fast fabrication of tissue constructs populated with stem cells.

To generate anisotropic fiber structure that mimics myocardial anisotropy, the tissue constructs were collected on a rotating mandrel. The fiber alignment was related to mandrel diameter and rotation speed. We found that a small diameter mandrel (≤ 5 cm) required a high rotation speed to achieve fiber alignment. However, the high rotation speed caused the electrosprayed MSCs to fly out of the mandrel. Using a bigger mandrel (diameter 11 cm) and a fairly high rotation speed (1500 rpm), the fabricated constructs showed an aligned structure (Figure 3B) and prevented MSCs to fly out of the mandrel. The degree of fiber alignment determined from SEM images was 72.5%.

3.4. Tissue construct mechanical properties

Biaxial mechanical properties were measured for the 8M and 30M constructs. Native porcine myocardium was used as a control. Both tissue constructs demonstrated a nonlinear anisotropic mechanical behavior (Figure 4). The fiber-preferred direction (PD) was stiffer than the cross fiber-preferred direction (XD). This behavior is similar to that of the native porcine myocardium (Figure 4A). Comparing the biaxial stress-strain curves of the two constructs with that of the porcine myocardium, the 8M construct was found to mimic the porcine myocardium more closely (Figure 4B).

Figure 5 shows areal strains at 10 kPa, strains at 10 kPa and hysteresis of the tissue constructs and native myocardium. The 8M construct exhibited the same areal strain as the porcine myocardium, while the 30M construct had significantly lower areal strain ($p<0.01$, Figure 5A). Both constructs and porcine myocardium had higher strain at 10 kPa (Figure 5B) in the fiber cross-preferred direction than in the fiber preferred direction. In the fiber cross-preferred direction, strain of the 8M construct was slightly higher than that of the porcine myocardium although no significant difference was observed ($p>0.1$). In contrast, the strain of 30M construct was significantly lower than those of the 8M construct and porcine myocardium ($p<0.01$). In the fiber preferred direction, both constructs displayed the same strain as the porcine myocardium. Comparing hysteresis of the constructs and porcine myocardium, the 30M construct had the highest hysteresis ($p<0.05$, Figure 5C), while the 8M construct showed a similar hysteresis to the porcine myocardium. These results demonstrated that biaxial mechanical behavior of the constructs was dependent on cell density. Controlling cell density enabled to fabricate constructs closely mimicking the anisotropic mechanical response of the native porcine myocardium.

3.5. MSCs growth and alignment in tissue constructs

The fabricated tissue constructs were cultured in spinner flasks for 7 days. Both tissue constructs, regardless of cell density, increased their dsDNA content (for live cells) during the culture (Figure 6). At day 7, the dsDNA content in both constructs was significantly higher than that at day 1 ($p<0.05$). Figure 7 represents typical CLSM images of MSCs within the constructs cultured under dynamic conditions. All images were taken at a depth of 45 μm. The MSCs were distributed evenly in the constructs during the culture period. The 30M construct showed higher cell density at each time point than the 8M constructs. However, MSCs in both tissue constructs assumed a round morphology. No obvious cell alignment was observed, even though the cells were situated in aligned tissue constructs.

To achieve 3-D cell alignment, the tissue constructs were cultured while being stretched along the fiber alignment direction. Three stretching strains namely 25%, 50% and 75% were applied. After 7 days of culture, 3-D cell alignment was observed in all the stretched tissue constructs (Figure 8). The degree of cell alignment was characterized by the cell anisotropic index. Cells in the tissue constructs stretched with a higher strain exhibited a higher anisotropic index. MSCs in the tissue construct without stretching had an anisotropic index of 0.14, while in tissue constructs subjected to 25%, 50% and 75% of strain had an anisotropic index of 1.82, 2.46 and 3.28, respectively.

3.5. MSCs differentiation in tissue constructs

To investigate whether the native-like microenvironment stimulated cardiac differentiation of MSCs, gene expression of the cells in the constructs was characterized. Makers for early cardiac differentiation (GATA4, MEF2C and Nkx2.5) were used. Compared to MSCs cultured on the tissue culture plate, cells in the tissue constructs without stretching slightly (∼2 times) but significantly upregulated MEF2C and Nkx2.5 expressions ($p<0.05$ for both expressions), and strongly upregulated GATA4 expression (increased more than 700 times, Figure 9). This result indicates that the cardiac-like structural and mechanical microenvironment substantially induced MSCs to undergo cardiac differentiation. The level of cardiac gene expression for the aligned MSCs was closely related to the anisotropic index. MSCs with an anisotropic index of 1.82 (with application of 25% strain) expressed GATA4 more than 7 times higher than those with an anisotropic index of 0.14 (without stretching); however, the MEF2C and Nkx2.5 expression levels were similar. When the anisotropic index was increased to 3.28, the expression levels of all three cardiac markers were remarkably increased, demonstrating that a high degree of cell alignment led to extensive cardiac differentiation.

The calcium channel gene is a vital component for the differentiated cells as this allows the cells to have electrophysiological properties. We found that expression of the calcium channel gene was upregulated in the tissue constructs (Figure 9C). MSCs with anisotropic indexes 0.14 and 1.82 demonstrated a low expression of this gene. However, when the anisotropic index was increased to 3.28, its expression was increased more than 450 times.

4. Discussion

Cardiac cell therapy has been widely accepted as an effective strategy for myocardium regeneration and cardiac function improvement of infarcted hearts [2,3]. Administration of stem cells into infarcted hearts has mainly focused on three approaches: injection of stem cells alone into the heart [50-52], injection of stem cells/injectable biomaterial into the heart [53,54], and patching a stem cell populated 3-D tissue construct onto the heart [46,55]. Compared to the injection approaches, the patching approach is more versatile in controlling properties of the tissue constructs.

The patching tissue constructs are often fabricated by combining a prefabricated scaffold with stem cells, followed by a period of culture to reach high cell density. This traditional tissue construct fabrication method is generally time-consuming as it basically relies on cell migration and proliferation to obtain high cell density. The cell migration and proliferation rates in 3-D constructs are largely affected by the scaffold properties, and nutrient and oxygen transport in the scaffolds. The highly cellularized tissue constructs can only be obtained when the scaffolds and culture conditions are appropriate. By combining electrospraying and electrospinning, we fabricated cellularized tissue constructs within 40 min. Since the fabricated tissue constructs are highly cellularized, they may be implanted directly onto the heart. These cellularized tissue constructs also provide an efficient way to investigate stem cell fate at the 3-D level. This work examined whether these cellularized tissue constructs mimicking structural and mechanical properties of the myocardium would

induce MSCs to differentiate into a cardiac lineage, and whether further mimicking the 3-D cell alignment of the myocardium would enhance cardiac differentiation.

4.1 Effect of electrical treatment on MSC survival, growth and multipotency

One concern raised in regard to electrospraying stem cells under high voltage is whether this treatment causes cell death, affects cell proliferation and multipotency. This motivated us to investigate the effect of high voltage on MSC. We found that electrospraying preserved more than 90% of viable MSCs even when the voltage was as high as 28 kV. The electrical treatment did not alter MSC proliferation kinetics even two passages after electrospraying (Figure 2A). Electrospraying also preserved MSC multipotentcy, as confirmed by mRNA expression and MSC differentiation (Figures 2B and C). At the mRNA level, MSCs showed representative markers corresponding to osteogenic and chondrogenic lineages. When cultured in the differentiation media, electrosprayed MSCs successfully differentiated into osteogenic, chondrogenic and adipogenic lineages. These three differentiations are commonly used to identify MSC multipotency [37,41]. Since MSCs are also capable of differentiating into cardiomyocytes [15-22], we speculated that the electrosprayed MSCs would also differentiate into cardiac lineage. The electrospraying voltage used to preserve MSC multipotency in this study was higher than that used by Sahoo et al., who reported that MSCs retained their multipotency only when the voltage was below 7.5 kV [56]. The discrepancy may be due to the different media used for electrospraying. Whereas we used a medium containing gelatin, Sahoo et al. employed a medium without gelatin. It is possible that gelatin has a protective effect on MSCs under high voltage.

4.2 Tissue construct myocardium-like structural properties

When fabricating tissue constructs for cardiac tissue engineering, mimicking structural properties of the myocardium would offer two benefits. First, it might allow the stem cells to arrange properly within the tissue constructs to develop a tissue resembling the structure of the native myocardium [24,32]. Second, the mechanical properties are related to structural properties. The alignment would allow the tissue constructs to show anisotropic mechanical properties that the native myocardium exhibits. Using electrospinning technique, the generated fibers had diameters ranging from 600-800 nm, within the size range of the collagen fibers in the myocardium [57]. Collecting the electrospun nanofibers on a rotating mandrel resulted in tissue constructs that resemble the aligned structure of the native myocardium (Figure 3).

4.3 Tissue construct myocardium-like mechanical properties

The importance of mimicking biomechanical properties of the cardiac muscle is three-fold. First, it might provide an appropriate biomechanical microenvironment for stem cells to differentiate in the heart. Various studies have demonstrated that stem cells differentiate into different lineages in response to matrix mechanical properties [58,59]. Second, the matching of mechanical properties would enable tissue constructs to respond synchronically with heart contraction and relaxation. This allows efficient mechanical signal transfer from the native myocardial environment to the stem cells, allowing them to differentiate into cardiac lineage in the native environment [32]. Third, simulating cardiac muscle properties would

effectively decrease wall stress of the infarcted hearts and thus attenuate cardiac dilation [60].

In fabrication of tissue constructs with myocardium-like mechanical properties, commonly used biodegradable polyesters, such as polylactide (PLA) and copolymers are not well-suited as they are relatively stiff. Scaffolds based on ECMs have limited mechanical properties, particularly in terms of their elasticity [46]. One of the options to fabricate cardiac tissue constructs is to use flexible and soft polymers [23,24]. The polyurethane used in this study is highly flexible and soft. It generated tissue constructs with mechanical properties close to those of the myocardium (Figures 4 and 5).

Biaxial testing demonstrated that the anisotropic structure allowed tissue constructs to possess anisotropic mechanical properties, where the fiber-preferred direction was stiffer than cross fiber-preferred direction. The biaxial mechanical properties were closely related to cell density. Control of cell density enabled fabrication of tissue constructs that closely mimicked the anisotropic stress-strain response of the native porcine myocardium. The 8M construct was found to mimic the porcine myocardium more closely (Figure 4). Further characterization demonstrated that areal strains at 10 kPa, strains at 10 kPa, and hysteresis of the 8M tissue construct, were the same as those of the native myocardium (Figure 5). The 30M construct showed a stiffer mechanical response than the 8M constructs in biaxial testing. This phenomenon is similar to that reported by Amoroso et al. [61], where incorporating smooth muscle cells into the scaffold stiffened the tissue constructs. A possible interpretation is that a cell serves as a fiber bonding site when it is adhered to two or more fibers. The elevated fiber-fiber interaction leads to an increase in stiffness. When the cell density is not high enough, cells are mostly distributed in pores and contact with each other. Thus, an increase in cell density does not significantly increase the number of cells bonding to multiple fibers and the mechanical properties remain unchanged. In contrast, when the cell density is high enough, the pores are saturated with cells; the rest of cells are forced to bond to multiple fibers causing a significant increase in bonding sites and, consequently, increased stiffness.

4.3 MSC growth and 3-D alignment in tissue constructs

The ability of MSC proliferation in the fabricated tissue constructs was evaluated by monitoring changes in the DNA content of live cells during culture. Figure 6 shows that the DNA content of both 8M and 30M tissue constructs was significantly increased at day 7, indicating that MSCs were able to proliferate in the tissue constructs. In addition, MSCs were distributed uniformly in the constructs during culture (Figure 7). These results demonstrated that the tissue constructs possessed a pore size suitable for cell growth. It is possible that having a larger pore size may allow the cells to proliferate at a greater rate. This could be achieved by refining the processing parameters such as polymer concentration and distance between the spinneret tip and collection mandrel [62]. However, increasing the pore size may change the biaxial mechanical properties of the tissue constructs.

Electrospun scaffolds are attractive for tissue engineering in that they resemble the scale and fibrous structure of the ECM. However, a critical disadvantage of these scaffolds is the effective placement of cells within the matrices. Electrospun scaffolds generally possess

small pores, limiting cellular migration and ingrowth within the scaffold. Previous attempts to increase scaffold pore size include incorporation of salt particles during the electrospinning process [63], co-electrospinning with water soluble polymer fibers that can be leached out subsequently [64], and making extremely sparse scaffolds [65]. However, the time period needed for cellular ingrowth in these scaffolds to achieve high cell density can take weeks [63-65]. To overcome these limitations, Yang et al. developed a layer-by-layer technique that sequentially electrospins nanofibers and electrosprays cells to form a tissue construct [66]. The disadvantage of this technique is that the formed layer-by-layer structure differs from that of the native tissue, where cells are intactly surrounded by ECM nanofibers. The simultaneous electrospinning/electrospraying technique employed in this study not only allowed us to incorporate high density of cells in the tissue constructs quickly, but also permitted the cells to be intactly surrounded by nanofibers and distributed uniformly in the construct.

MSCs assumed a round morphology in the fabricated tissue constructs (Figure 7). The aligned fibers did not guide 3-D alignment of MSCs. This is different from 2-D culture, where cells on the scaffold surface often align along the aligned fibers [31]. This implies that an aligned fibrous scaffold does not necessarily guide 3-D cell alignment. To achieve 3-D cell alignment, we stretched tissue constructs statically during the culture. It was found that a 25% or higher strain could induce 3-D cell alignment (Figure 8). Higher levels of strain led to a higher degree of cell alignment. Stretching induced cell alignment may be the result of compression mediated deformation [61]. Stretching causes a decrease in space between fibers compared to unstretched tissue constructs. This forces the cells to adjust their morphology to fit in the decreased space and form an aligned structure. An increase in stretching strain leads to a further decrease of space, resulting in a higher degree of cell alignment. Compression mediated deformation has previously been observed in aortic valve interstitial cells [61].

4.4 Effect of 3-D cell alignment on MSC cardiac differentiation

When implanting MSC-populated tissue constructs in hearts, cardiac differentiation is needed to guarantee myocardial regeneration and heart function improvement. Cardiac differentiation can be induced by local biochemical and biomechanical aspects of the native myocardial environment [44,45]. However, the tissue construct itself may also encourage MSC differentiation. The hypothesis in this study was that biomimetic tissue constructs that mimic the structural and mechanical properties of the myocardium may provide a native-like microenvironment to guide MSCs differentiation into a cardiac lineage. Real time RT-PCR results (Figure 9) showed that the biomimetic tissue constructs substantially induced cardiac differentiation of MSCs. The expression level of cardiac markers MEF2C and Nkx2.5 was increased ∼2 times, and the expression level of GATA4 was largely increased. This implies that the tissue constructs recapitulating myocardial structural and mechanical properties stimulated cardiac differentiation of MSCs, although the differentiation is not extensive.

We further hypothesized that mimicking 3-D cell alignment in the myocardium may enhance cardiac differentiation of MSCs. The aligned MSCs with an anisotropic index of 1.82 (with application of 25% strain) showed a remarkably higher level of GATA4

expression than the MSCs with an anisotropic index of 0.14 in the unstretched tissue constructs (Figure 9). However, their MEF2C and Nkx2.5 expressions were similar. This indicates that even a 25% strain did not allow the MSCs to have a degree of alignment that could stimulate extensive cardiac differentiation. Remarkable cardiac differentiation was found when the MSCs had an anisotropic index of 3.82, which was achieved by 75% of strain. The expression levels of all three cardiac markers were remarkably increased, compared to MSCs with an anisotropic index of 0.14. Interestingly, the MSCs with an anisotropic index of 3.28 also showed a high expression level of CACNA1c, a marker for calcium channel. Calcium channel is a critical component of normal physiology of the cardiomyocyte. The contraction/relaxation of cardiomyocyte is triggered by calcium ions flowing across the cell membrane.

The relationship between cell alignment and cardiac differentiation of MSCs in this report may to some extent explain the outcome of many in vivo studies, where a limited proportion of the injected MSCs differentiated into cardiomyocytes [4-9]. A typical heartbeat cycle experiences ∼20% of strain [24]. Based on the current study, this level of strain may not be enough to guide the injected MSCs towards a high degree of alignment, and thus cannot induce extensive cardiac differentiation. Previous in vivo studies and our own work suggest that pre-differentiation of MSCs in vitro into cardiomyocytes may result in a greater degree of cardiac regeneration than simply injecting un-differentiated MSCs into the heart.

The role of cell alignment in differentiation has been observed in other studies. Lim et al. found that aligned adult neural stem cells cultured on aligned polycaprolactone fibers effectively upregulated neuronal differentiation [67]. Bashur et al. studied the differentiation of MSCs cultured on the surface of aligned polyurethane fibers [68]. The aligned MSCs exhibited a slightly upregulated mRNA expression for tendon fibroblasts. However, the polyurethane used in the study had mechanical properties that did not match those of the native tendon (∼50 times lower). It should be pointed out that these studies were limited to 2-D, whereby cells were cultured on the scaffold surface. These cells may behave differently from those in the 3-D due to a different microenvironment [58,59]. Our report investigated stem cell differentiation not only in 3-D but also in a mechanical and structural microenvironment that mimicked that of the myocardium. The developed tissue constructs may be used as an ex vivo microenvironment to investigate differentiation of different types of stem cell for cardiac therapy.

5. Conclusions

In this study we fabricated tissue constructs mimicking nanofibrous and anisotropic structure, and mechanical properties of the myocardium. These tissue constructs were found to substantially stimulate cardiac differentiation of MSCs. Enhanced cardiac differentiation was achieved by 3-D alignment of cells in the tissue constructs to reach a high degree of cell alignment. These tissue constructs have the potential to serve as patches for cardiac regeneration. This work represents a new approach to improve MSC cardiac differentiation in a 3-D structure, without using biochemicals or co-culturing with other cells. This work also demonstrates that stem cells may differentiate into the specific lineage of a target tissue

in vitro in a tissue construct that mimics structural and mechanical properties, and cellular organization of the target tissue.

Acknowledgments

We thank Dr. Andre Palmer in Department of Chemical and Biomolecular Engineering at The Ohio State University for help in real time RT-PCR characterization. We also thank Dr. Peter Anderson in Department of Materials Science and Engineering at The Ohio State University for valuable discussion. This work was supported by National Science Foundation (DMR1006734), National Institutes of Health (RC2AG036559 and R01HL096524) and Institute for Materials Research at The Ohio State University.

References

1. Rubin, R.; Strayer, DS.; Rubin, E. Rubin's Pathology: clinicopathologic foundations of medicine. 4th. Lippincott Williams & Wilkins; 2008.
2. Flynn A, O'Brien T. Stem cell therapy for cardiac disease. Expert Opin Biol Ther. 2011; 11:177–87. [PubMed: 21219235]
3. Forrester JS, Makkar RR, Marbán E. Long-term outcome of stem cell therapy for acute myocardial infarction: right results, wrong reasons. J Am Coll Cardiol. 2009; 53:2270–2. [PubMed: 19520250]
4. Miyahara Y, Nagaya N, Kataoka M, Yanagawa B, Tanaka K, Hao H, et al. Monolayered mesenchymal stem cells repair scarred myocardium after myocardial infarction. Nat Med. 2006; 12:459–65. [PubMed: 16582917]
5. Quevedo HC, Hatzistergos KE, Oskouei BN, Feigenbaum GS, Rodriguez JE, Valdes D, et al. Allogeneic mesenchymal stem cells restore cardiac function in chronic ischemic cardiomyopathy via trilineage differentiating capacity. Proc Natl Acad Sci U S A. 2009; 106:14022–7. [PubMed: 19666564]
6. Toma C, Pittenger MF, Cahill KS, Byrne BJ, Kessler PD. Human mesenchymal stem cells differentiate to a cardiomyocyte phenotype in the adult murine heart. Circulation. 2002; 105:93–98. [PubMed: 11772882]
7. Cho J, Zhai P, Maejima Y, Sadoshima J. Myocardial injection with GSK-3β-overexpressing bone marrow-derived mesenchymal stem cells attenuates cardiac dysfunction after myocardial infarction. Circ Res. 2011; 108(4):478–89. [PubMed: 21233455]
8. Nagaya N, Kangawa K, Itoh T, Iwase T, Murakami S, Miyahara Y, et al. Transplantation of mesenchymal stem cells improves cardiac function in a rat model of dilated cardiomyopathy. Circulation. 2005; 112(8):1128–35. [PubMed: 16103243]
9. Song H, Hwang HJ, Chang W, Song BW, Cha MJ, Kim IK, et al. Cardiomyocytes from phorbol myristate acetate-activated mesenchymal stem cells restore electromechanical function in infarcted rat hearts. Proc Natl Acad Sci U S A. 2011; 108(1):296–301. [PubMed: 21173226]
10. Bel A, Planat-Bernard V, Saito A, Bonnevie L, Bellamy V, Sabbah L, et al. Composite cell sheets: a further step toward safe and effective myocardial regeneration by cardiac progenitors derived from embryonic stem cells. Circulation. 2010; 122:S118–23. [PubMed: 20837902]
11. Nelson TJ, Martinez-Fernandez A, Yamada S, Perez-Terzic C, Ikeda Y, Terzic A. Repair of acute myocardial infarction by human stemness factors induced pluripotent stem cells. Circulation. 2009; 120:408–16. [PubMed: 19620500]
12. Bailey B, Izarra A, Alvarez R, Fischer KM, Cottage CT, Quijada P, et al. Cardiac stem cell genetic engineering using the αMHC promoter. Regen Med. 2009; 4:823–33. [PubMed: 19903002]
13. Davis DR, Zhang Y, Smith RR, Cheng K, Terrovitis J, Malliaras K, et al. Validation of the cardiosphere method to culture cardiac progenitor cells from myocardial tissue. PloS one. 2009; 4:e7195. [PubMed: 19779618]
14. Smith RR, Barile L, Cho HC, Leppo MK, Hare JM, Messina E, et al. Regenerative potential of cardiosphere-derived cells expanded from percutaneous endomyocardial biopsy specimens. Circulation. 2007; 115:896–908. [PubMed: 17283259]
15. Hare JM. Translational development of mesenchymal stem cell therapy for cardiovascular diseases. Tex Heart Inst J. 2009; 36(2):145–147. [PubMed: 19436809]

16. Ripa RS, Haack-Sørensen M, Wang Y, Jørgensen E, Mortensen S, Bindslev L, et al. Bone marrow derived mesenchymal cell mobilization by granulocyte-colony stimulating factor after acute myocardial infarction: results from the Stem Cells in Myocardial Infarction (STEMMI) trial. Circulation. 2007; 116:I24–30. [PubMed: 17846310]
17. Chen S, Liu Z, Tian N, Zhang J, Yei F, Duan B, et al. Intracoronary transplantation of autologous bone marrow mesenchymal stem cells for ischemic cardiomyopathy due to isolated chronic occluded left anterior descending artery. J Invasive Cardiol. 2006; 18:552–556. [PubMed: 17090821]
18. Feng C, Zhu J, Zhao L, Lu T, Zhang W, Liu Z, et al. Suberoylanilide hydroxamic acid promotes cardiomyocyte differentiation of rat mesenchymal stem cells. Exp Cell Res. 2009; 315:3044–51. [PubMed: 19445929]
19. Hakuno D, Fukuda K, Makino S, Konishi F, Tomita Y, Manabe T, et al. Bone marrow-derived regenerated cardiomyocytes (CMG Cells) express functional adrenergic and muscarinic receptors. Circulation. 2002; 105(3):380–6. [PubMed: 11804996]
20. Yang MC, Wang SS, Chou NK, Chi NH, Huang YY, Chang YL, et al. The cardiomyogenic differentiation of rat mesenchymal stem cells on silk fibroin-polysaccharide cardiac patches in vitro. Biomaterials. 2009; 30(22):3757–65. [PubMed: 19410289]
21. Cho J, Rameshwar P, Sadoshima J. Distinct roles of glycogen synthase kinase (GSK)-3alpha and GSK-3beta in mediating cardiomyocyte differentiation in murine bone marrow-derived mesenchymal stem cells. J Biol Chem. 2009; 284(52):36647–58. [PubMed: 19858210]
22. Pijnappels DA, Schalij MJ, Ramkisoensing AA, van Tuyn J, de Vries AA, van der Laarse A, et al. Forced alignment of mesenchymal stem cells undergoing cardiomyogenic differentiation affects functional integration with cardiomyocyte cultures. Circ Res. 2008; 103(2):167–76. [PubMed: 18556577]
23. Radisic M, Park H, Chen F, Salazar-Lazzaro JE, Wang Y, Dennis R, et al. Biomimetic approach to cardiac tissue engineering: oxygen carriers and channeled scaffolds. Tissue Eng. 2006; 12:2077–91. [PubMed: 16968150]
24. Engelmayr GC Jr, Cheng M, Bettinger CJ, Borenstein JT, Langer R, Freed LE. Accordion-like honeycombs for tissue engineering of cardiac anisotropy. Nat Mater. 2008; 7:1003–10. [PubMed: 18978786]
25. Radisic M, Park H, Shing H, Consi T, Schoen FJ, Langer R, et al. Functional assembly of engineered myocardium by electrical stimulation of cardiac myocytes cultured on scaffolds. Proc Natl Acad Sci U S A. 2004; 101:18129–34. [PubMed: 15604141]
26. Zimmermann WH, Melnychenko I, Wasmeier G, Didié M, Naito H, Nixdorff U, et al. Engineered heart tissue grafts improve systolic and diastolic function in infarct rat hearts. Nat Med. 2006; 12:452–8. [PubMed: 16582915]
27. Simpson D, Liu H, Fan TH, Nerem R, Dudley SC Jr. A tissue engineering approach to progenitor cell delivery results in significant cell engraftment and improved myocardial remodeling. Stem Cells. 2007; 25:2350–7. [PubMed: 17525236]
28. Dvir T, Kedem A, Ruvinov E, Levy O, Freeman I, Landa N, et al. Prevascularization of cardiac patch on the omentum improves its therapeutic outcome. Proc Natl Acad Sci U S A. 2009; 106:14990–5. [PubMed: 19706385]
29. Yang MC, Chi NH, Chou NK, Huang YY, Chung TW, Chang YL, Liu HC, Shieh MJ, Wang SS. The influence of rat mesenchymal stem cell CD44 surface markers on cell growth, fibronectin expression, and cardiomyogenic differentiation on silk fibroin - Hyaluronic acid cardiac patches. Biomaterials. 2010; 31(5):854–62. [PubMed: 19857893]
30. Fujimoto KL, Tobita K, Merryman WD, Guan J, Momoi N, Stolz DB, et al. An elastic, biodegradable cardiac patch induces contractile smooth muscle and improves cardiac remodeling and function in subacute myocardial infarction. J Am Coll Cardiol. 2007; 49:2292–300. [PubMed: 17560295]
31. Rockwood DN, Akins RE Jr, Parrag IC, Woodhouse KA, Rabolt JF. Culture on electrospun polyurethane scaffolds decreases atrial natriuretic peptide expression by cardiomyocytes in vitro. Biomaterials. 2008; 29:4783–91. [PubMed: 18823659]

32. Wang F, Guan J. Cellular cardiomyoplasty and cardiac tissue engineering for myocardial therapy. Adv Drug Deliv Rev. 2010; 62:784–97. [PubMed: 20214939]
33. Wang F, Li Z, Lannutti JL, Wagner WR, Guan J. Synthesis, characterization and surface modification of low moduli poly(ether carbonate urethane)ureas for soft tissue engineering. Acta Biomater. 2009; 5:2901–12. [PubMed: 19433136]
34. Guan J, Sacks MS, Beckman EJ, Wagner WR. Biodegradable poly(ether ester urethane)urea elastomers based on poly(ether ester) triblock copolymers and putrescine: synthesis, characterization and cytocompatibility. Biomaterials. 2004; 25:85–96. [PubMed: 14580912]
35. Guan J, Sacks MS, Beckman EJ, Wagner WR. Synthesis, characterization, and cytocompatibility of elastomeric, biodegradable poly(ester urethane)ureas based on polycaprolactone and putrescine. J Biomed Mater Res. 2002; 61:493–503. [PubMed: 12115475]
36. Wang F, Li Z, Khan M, Tamama K, Kuppusamy P, Wagner WR, et al. Injectable, rapid gelling and highly flexible hydrogel composites as growth factor and cell carriers. Acta Biomater. 2010; 6:1978–91. [PubMed: 20004745]
37. Song L, Tuan RS. Transdifferentiation potential of human mesenchymal stem cells derived from bone marrow. FASEB J. 2004; 18:980–2. [PubMed: 15084518]
38. Wang F, Li Z, Tamama K, Sen CK, Guan J. Fabrication and characterization of prosurvival growth factor releasing, anisotropic scaffolds for enhanced mesenchymal stem cell survival/growth and orientation. Biomacromolecules. 2009; 10:2609–18. [PubMed: 19689108]
39. Cohen J, Zaleski KL, Nourissat G, Julien TP, Randolph MA, Yaremchuk MJ. Survival of porcine mesenchymal stem cells over the alginate recovered cellular method. J Biomed Mater Res A. 2011; 96:93–9. [PubMed: 21105156]
40. Yow SZ, Quek CH, Yim KF, Lim CT, Leong KW. Collagen-based fibrous scaffold for spatial organization of encapsulated and seeded human mesenchymal stem cells. Biomaterials. 2009; 30:1133–42. [PubMed: 19041132]
41. Song L, Webb NE, Song Y, Tuan RS. Identification and functional analysis of candidate genes regulating mesenchymal stem cell self-renewal and multipotency. Stem Cells. 2006; 24:1707–18. [PubMed: 16574750]
42. Stankus JJ, Guan J, Fujimoto K, Wagner WR. Microintegrating smooth muscle cells into a biodegradable, elastomeric fiber matrix. Biomaterials. 2006; 27:735–44. [PubMed: 16095685]
43. Li WJ, Mauck RL, Cooper JA, Yuan X, Tuan RS. Engineering controllable anisotropy in electrospun biodegradable nanofibrous scaffolds for musculoskeletal tissue engineering. J Biomech. 2007; 40:1686–93. [PubMed: 17056048]
44. Courtney T, Sacks MS, Stankus J, Guan J, Wagner WR. Design and analysis of tissue engineering scaffolds that mimic soft tissue mechanical anisotropy. Biomaterials. 2006; 27:3631–8. [PubMed: 16545867]
45. Grashow JS, Yoganathan AP, Sacks MS. Biaixal stress-stretch behavior of the mitral valve anterior leaflet at physiologic strain rates. Ann Biomed Eng. 2006; 34:315–25. [PubMed: 16450193]
46. Wang B, Borazjani A, Tahai M, Curry AL, Simionescu DT, Guan J, et al. Fabrication of cardiac patch with decellularized porcine myocardial scaffold and bone marrow mononuclear cells. J Biomed Mater Res A. 2010; 94:1100–10. [PubMed: 20694977]
47. Li Z, Wang F, Roy S, Sen CK, Guan J. Injectable, highly flexible, and thermosensitive hydrogels capable of delivering superoxide dismutase. Biomacromolecules. 2009; 10:3306–16. [PubMed: 19919046]
48. Ng CP, Hinz B, Swartz MA. Interstitial fluid flow induces myofibroblast differentiation and collagen alignment in vitro. J Cell Sci. 2005; 118:4731–9. [PubMed: 16188933]
49. Li Z, Guo X, Matsushita S, Guan J. Differentiation of cardiosphere-derived cells into a mature cardiac lineage using biodegradable poly(N-isopropylacrylamide) hydrogels. Biomaterials. 2011; 32:3220–32. [PubMed: 21296413]
50. Kraehenbuehl TP, Ferreira LS, Hayward AM, Nahrendorf M, van der Vlies AJ, Vasile E, et al. Human embryonic stem cell-derived microvascular grafts for cardiac tissue preservation after myocardial infarction. Biomaterials. 2011; 32:1102–9. [PubMed: 21035182]

51. Nelson TJ, Martinez-Fernandez A, Yamada S, Perez-Terzic C, Ikeda Y, Terzic A. Repair of acute myocardial infarction by human stemness factors induced pluripotent stem cells. Circulation. 2009; 120:408–16. [PubMed: 19620500]
52. Smith RR, Barile L, Cho HC, Leppo MK, Hare JM, Messina E, et al. Regenerative potential of cardiosphere-derived cells expanded from percutaneous endomyocardial biopsy specimens. Circulation. 2007; 115:896–908. [PubMed: 17283259]
53. Ryu JH, Kim IK, Cho SW. Implantation of bone marrow mononuclear cells using injectable fibrin matrix enhances neovascularization in infarcted myocardium. Biomaterials. 2005; 26:319–26. [PubMed: 15262474]
54. Zhang G, Hu Q, Braunlin EA, Suggs LJ, Zhang J. Enhancing efficacy of stem cell transplantation to the heart with a PEGylated fibrin biomatrix. Tissue Eng Part A. 2008; 14:1025–36. [PubMed: 18476809]
55. Huang CC, Liao CK, Yang MJ, Chen CH, Hwang SM, Hung YW, et al. A strategy for fabrication of a three-dimensional tissue construct containing uniformly distributed embryoid body-derived cells as a cardiac patch. Biomaterials. 2010; 31:6218–27. [PubMed: 20537702]
56. Sahoo S, Lee WC, Goh JC, Toh SL. Bio-electrospraying: A potentially safe technique for delivering progenitor cells. Biotechnol Bioeng. 2010; 106(4):690–8. [PubMed: 20229515]
57. Weis SM, Emery JL, Becker KD, McBride DJ Jr, Omens JH, McCulloch AD. Myocardial mechanics and collagen structure in the osteogenesis imperfecta murine (oim). Circ Res. 2000; 87:663–9. [PubMed: 11029401]
58. Tse JR, Engler AJ. Stiffness gradients mimicking in vivo tissue variation regulate mesenchymal stem cell fate. PLoS One. 2011; 6(1):e15978. [PubMed: 21246050]
59. Engler AJ, Sen S, Sweeney HL, Discher DE. Matrix elasticity directs stem cell lineage specification. Cell. 2006; 126:677–89. [PubMed: 16923388]
60. Wall ST, Walker JC, Healy KE, Ratcliffe MB, Guccione JM. Theoretical impact of the injection of material into the myocardium - A finite element model simulation. Circulation. 2006; 114:2627–35. [PubMed: 17130342]
61. Amoroso NJ, D'Amore A, Hong Y, Wagner WR, Sacks MS. Elastomeric electrospun polyurethane scaffolds: the interrelationship between fabrication conditions, fiber topology, and mechanical properties. Adv Mater. 2011; 23:106–11. [PubMed: 20979240]
62. Greiner A, Wendorff JH. Electrospinning: A fascinating method for the preparation of ultrathin fibres. Angew Chem-Int Edit. 2007; 46:5670–703.
63. Nam J, Huang Y, Agarwal S, Lannutti JJ. Improved cellular infiltration in electrospun fiber via engineered porosity. Tissue Eng. 2007; 13:2249–57. [PubMed: 17536926]
64. Baker BM, Gee AO, Metter RB, Nathan AS, Marklein RA, Burdick JA, et al. The potential to improve cell infiltration in composite fiber-aligned electrospun scaffolds by the selective removal of sacrificial fibers. Biomaterials. 2008; 29:2348–58. [PubMed: 18313138]
65. Blakeney BA, Tambralli A, Anderson JM, Andukuri A, Lim DJ, Dean DR, et al. Cell infiltration and growth in a low density, uncompressed three-dimensional electrospun nanofibrous scaffold. Biomaterials. 2011; 32:1583–90. [PubMed: 21112625]
66. Yang X, Shah JD, Wang H. Nanofiber enabled layer-by-layer approach toward three-dimensional tissue formation. Tissue Eng Part A. 2009; 15:945–56. [PubMed: 18788981]
67. Lim SH, Liu XY, Song H, Yarema KJ, Mao HQ. The effect of nanofiber-guided cell alignment on the preferential differentiation of neural stem cells. Biomaterials. 2010; 31(34):9031–9. [PubMed: 20797783]
68. Bashur CA, Shaffer RD, Dahlgren LA, Guelcher SA, Goldstein AS. Effect of fiber diameter and alignment of electrospun polyurethane meshes on mesenchymal progenitor cells. Tissue Eng Part A. 2009; 15(9):2435–45. [PubMed: 19292650]

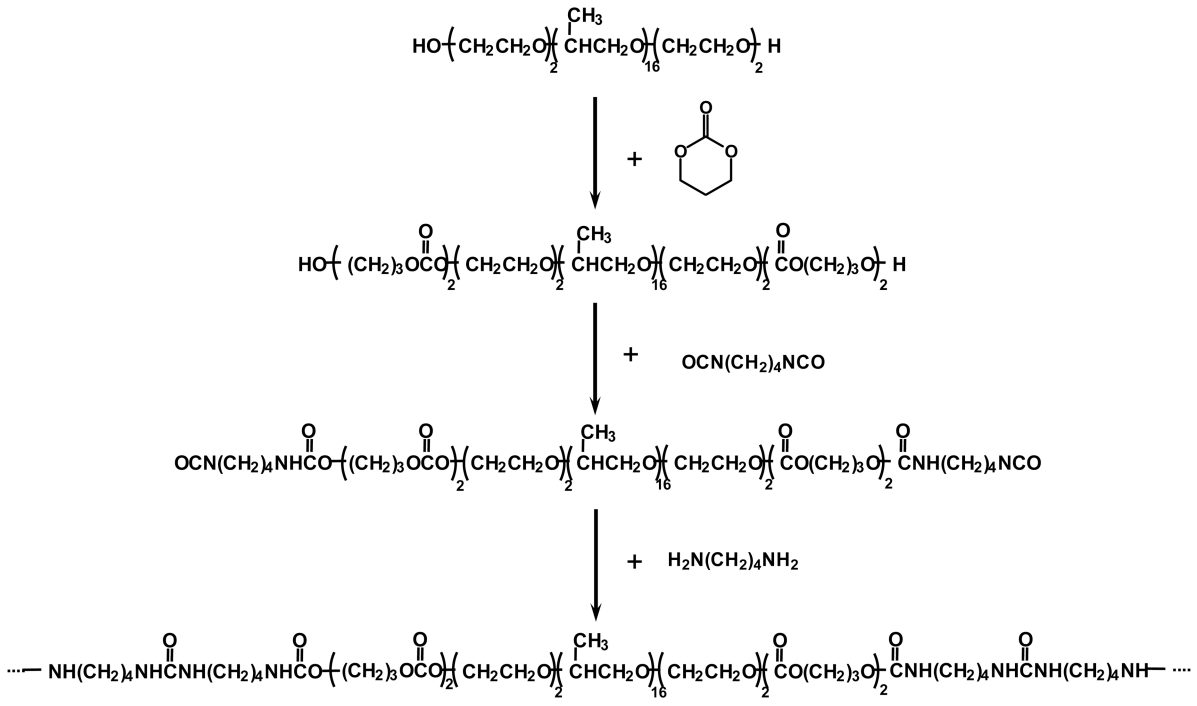

Figure 1.
Scheme of PECUU synthesis.

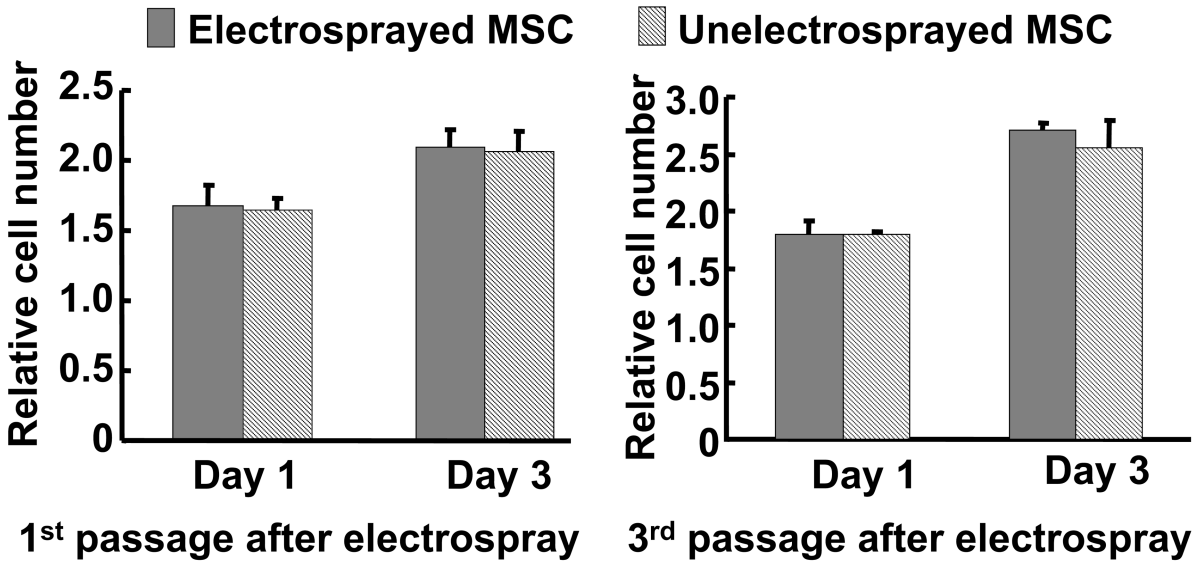

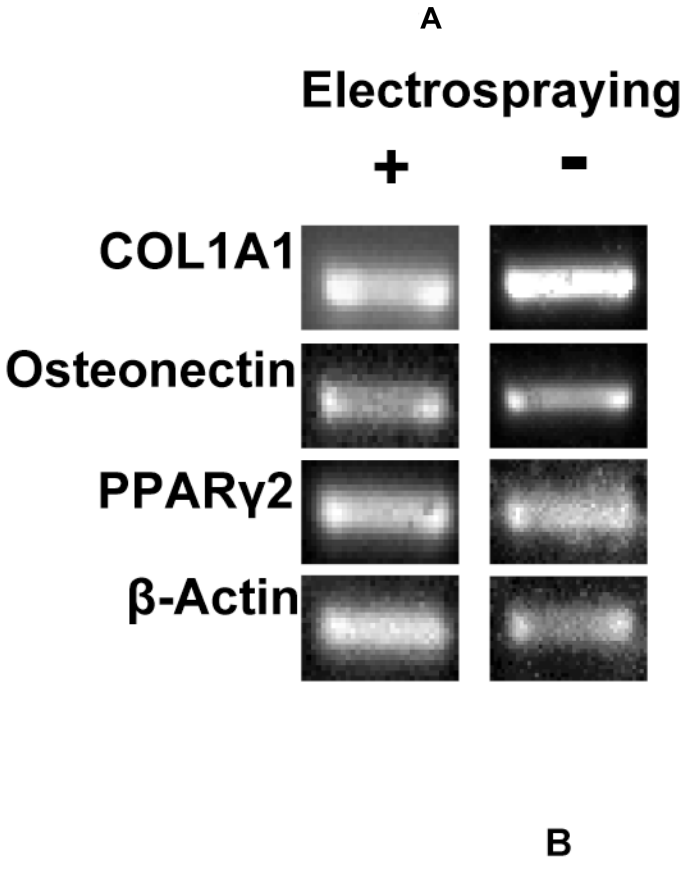

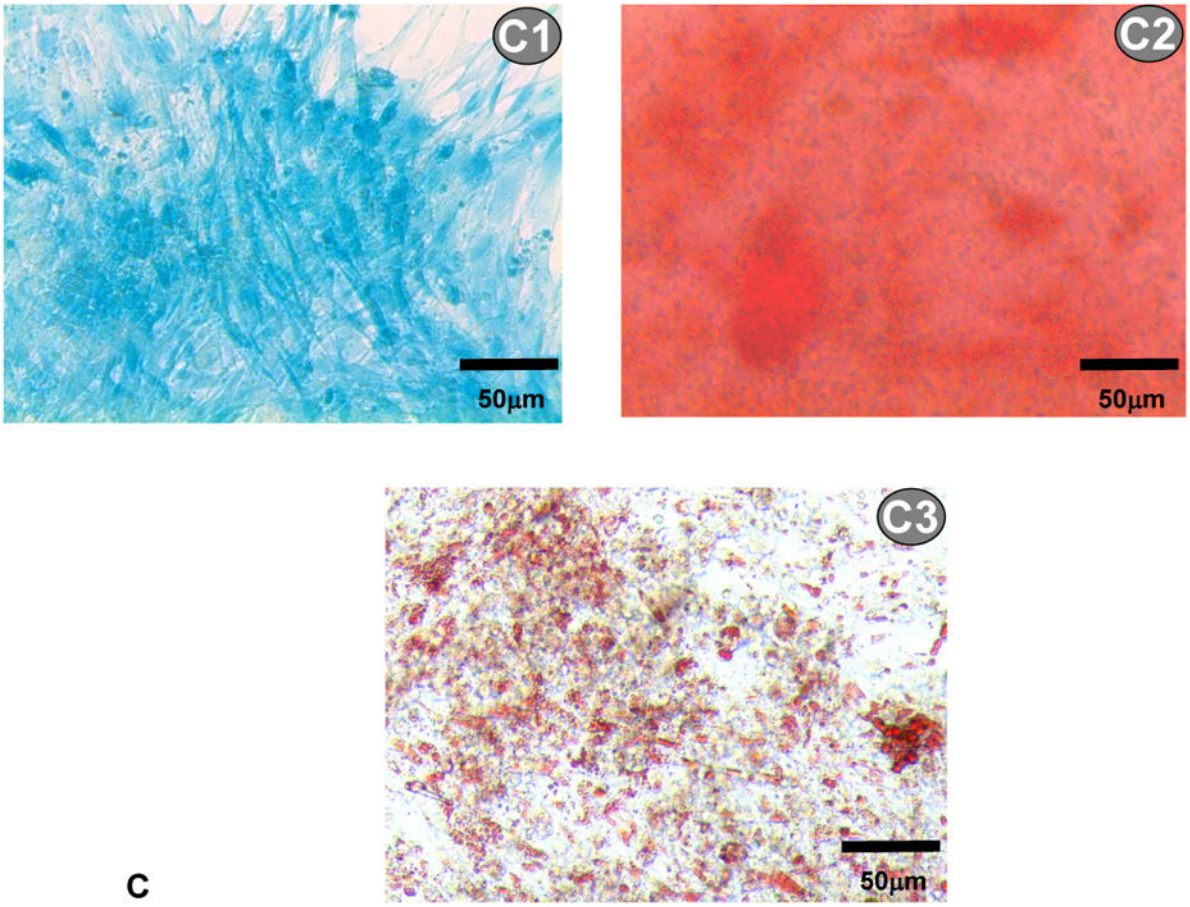

Figure 2.

(A) Growth kinetics of electrosprayed MSCs. Cell growth was quantified by MTT assay; (B) gene expression of osteogenic and adipogenic markers of electrosprayed and non-electrosprayed MSCs. Note that these genes were selected to confirm MSC multipotency; and (C) differentiation of electrosprayed MSCs. C1 is Alcian blue staining for chondrogenesis. C2 is alizarin red staining for osteogenesis. C3 is Oil Red O staining for adipogenesis.

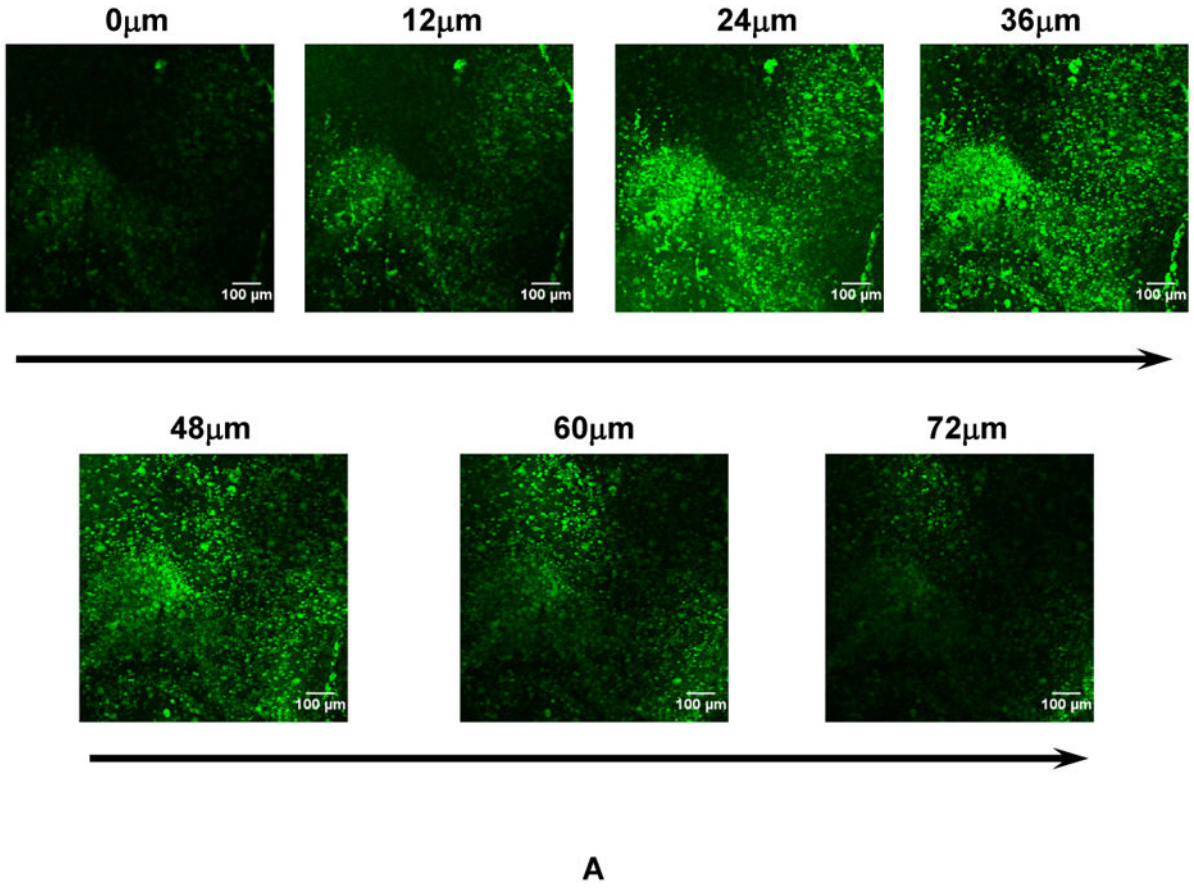

A

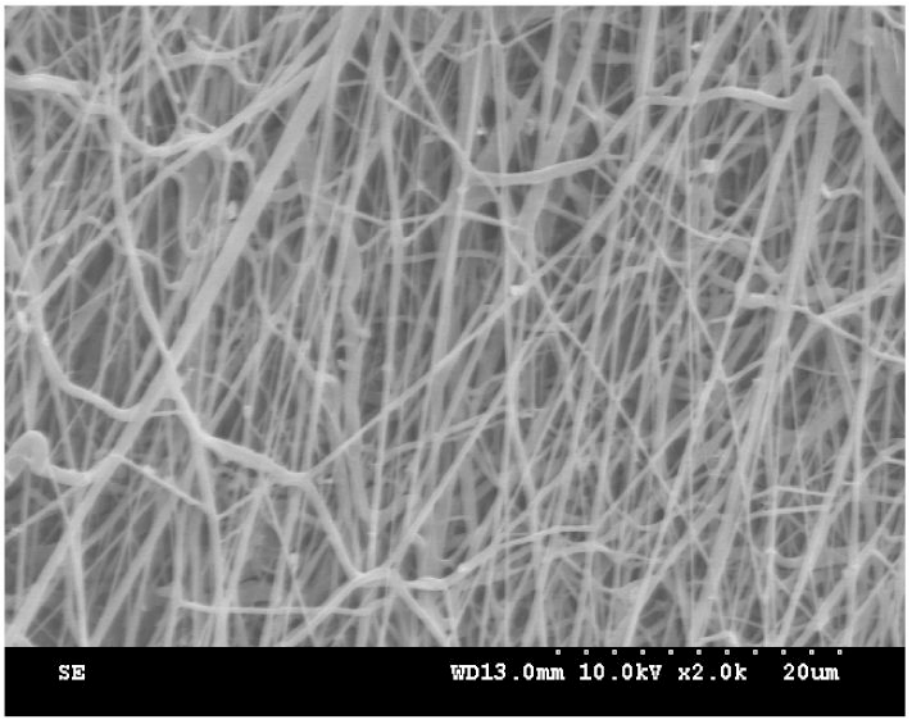

B

Figure 3.

(A) Z-stack confocal images of the tissue construct at different depth after one day of culture. Cells were stained with live cell stain CMFDA. (B) Surface topology of the tissue construct. The tissue construct was immersed in PBS for 1 day to completely remove gelatin and cells on the surface. This process allowed better imaging fibers, which otherwise can not be clearly imaged due to the interference of gelatin and cells.

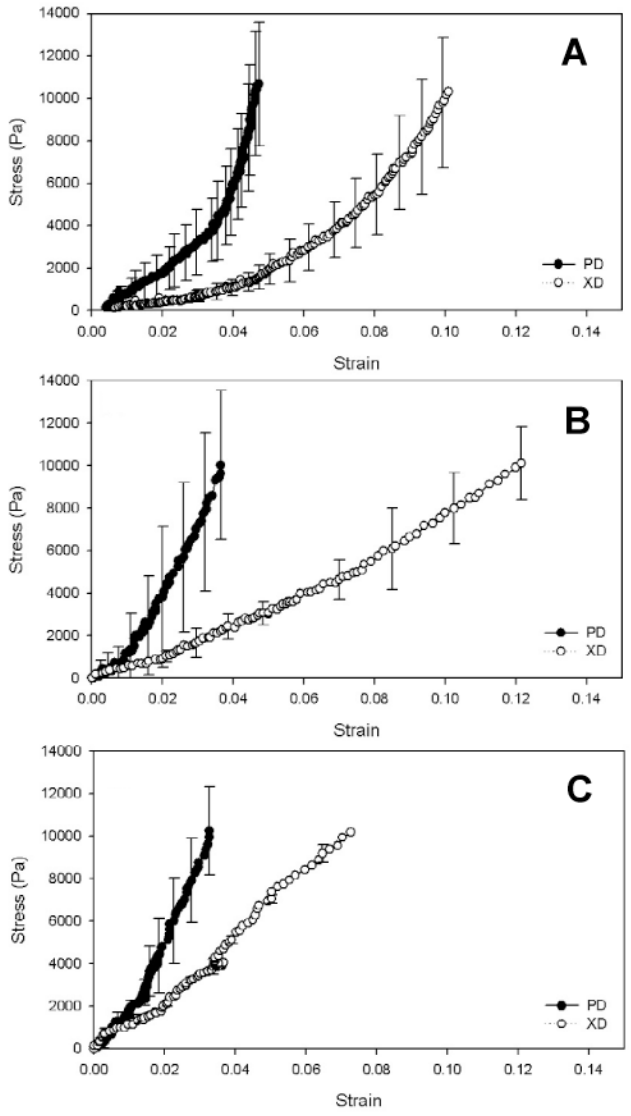

Figure 4.

Biaxial stress-strain curves of the porcine myocardium (A), 8M (B) and 30M (C) tissue constructs.

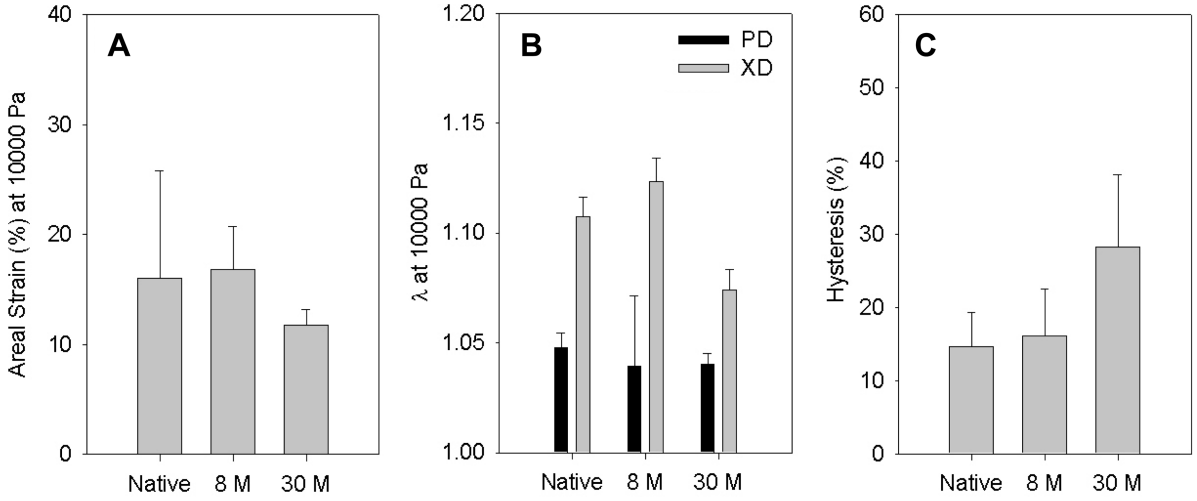

Figure 5.

Areal strain (A), strain at 10 kPa (B) and hysteresis (C) of the porcine myocardium and tissue constructs (8M and 30M).

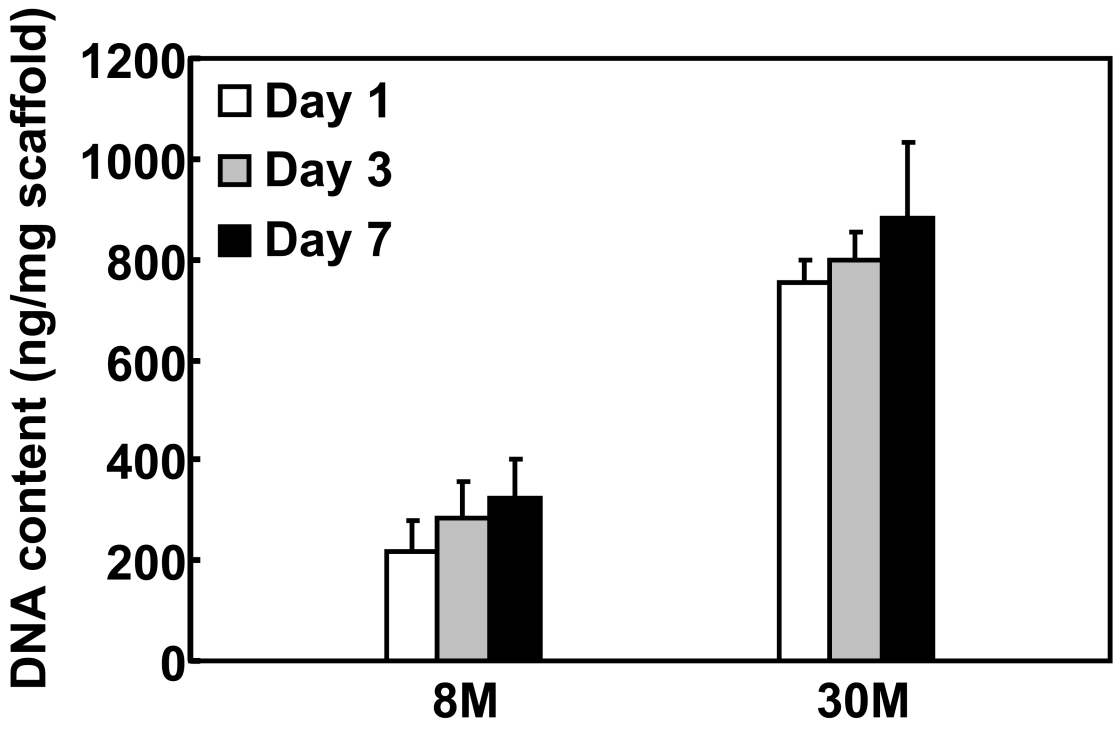

Figure 6.
dsDNA content (for live cells) of tissue constructs with different cell density after 1, 3 and 7 days of culture.

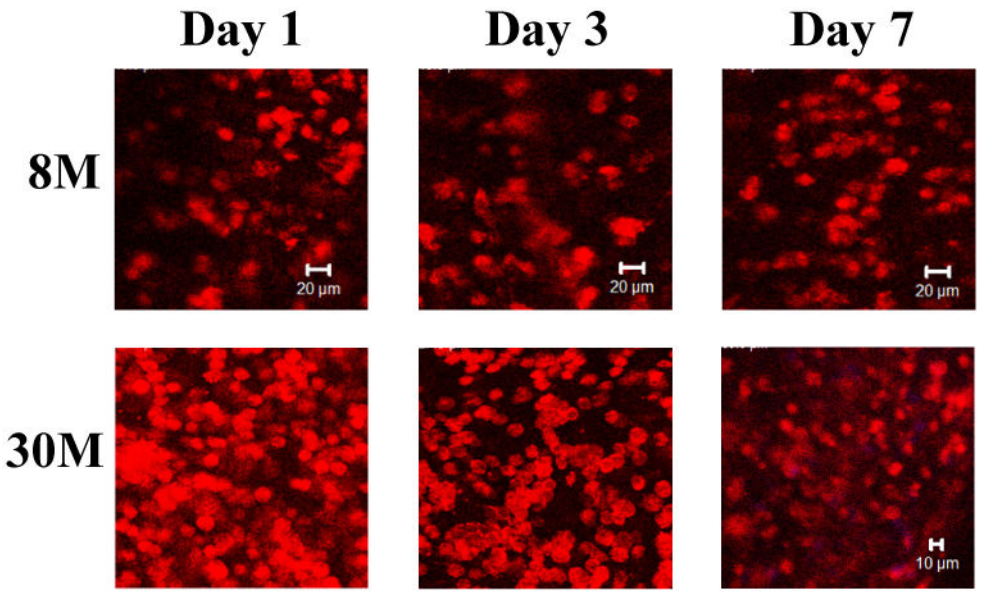

Figure 7.

Representative Z-stack confocal images of MSCs in the 8M and 30M tissue constructs at day 1, 3 and 7. All images were taken at a depth of 45 μm. The tissue constructs were cultured dynamically in spinner flasks. Cells were stained with rhodamine-phalloidin for F-actin.

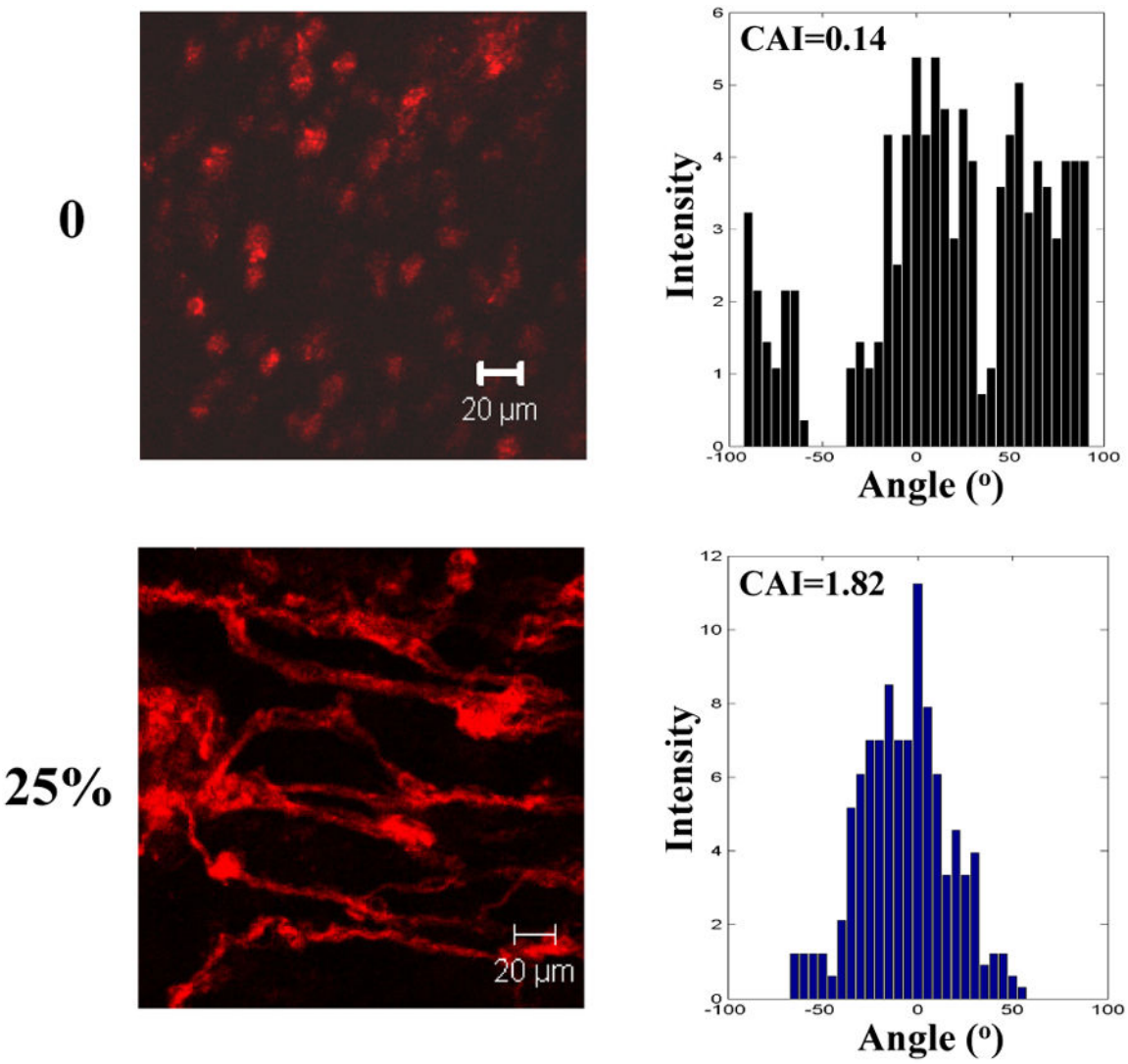

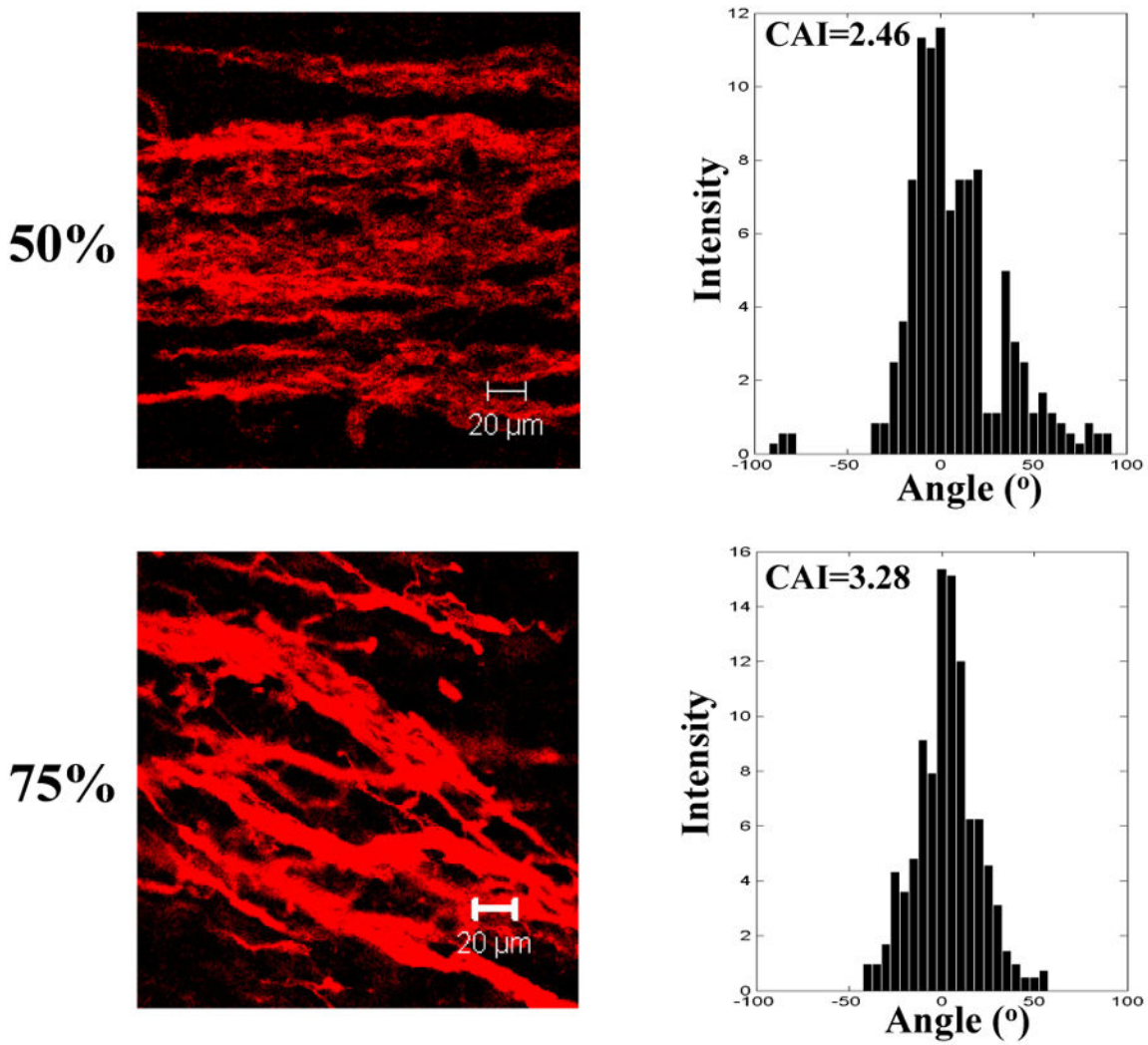

Figure 8.

Representative Z-stack confocal images and cell anisotropic index (CAI) of MSCs in the tissue constructs stretched at different strains (0, 25, 50 and 75%) on day 7. F-actins of the cells were stained with rhodamine phalloidin. All images were taken at a depth of 45 μm.

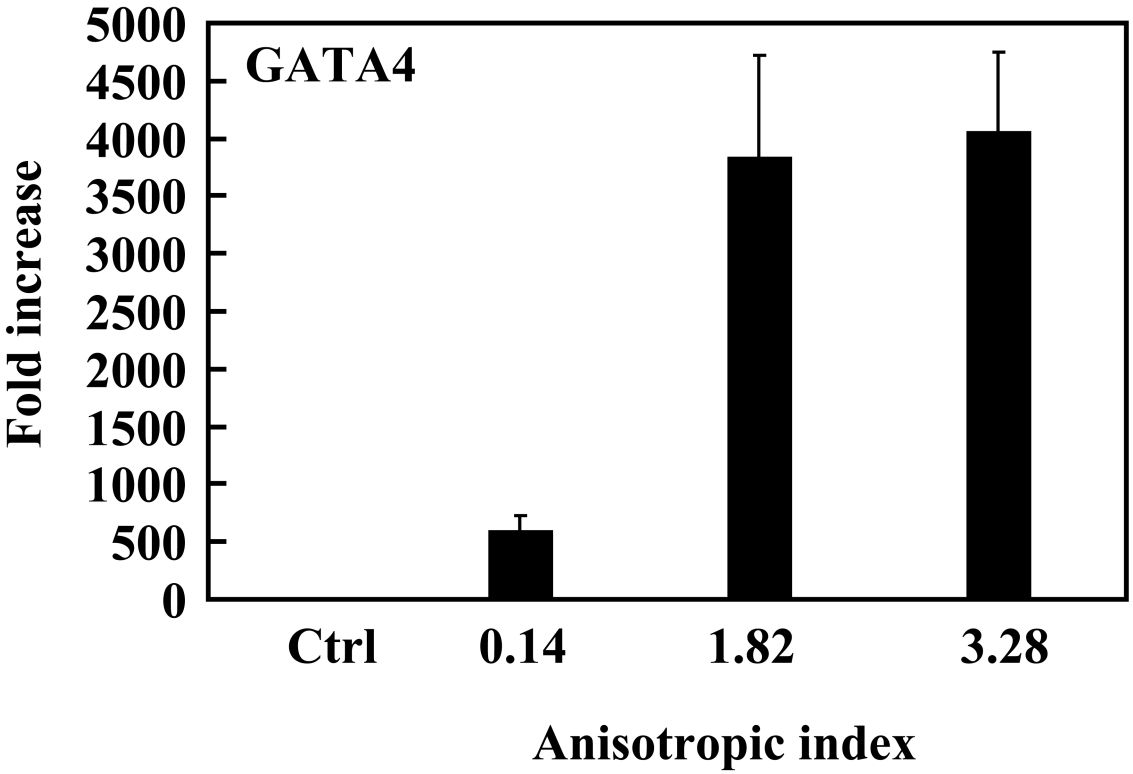

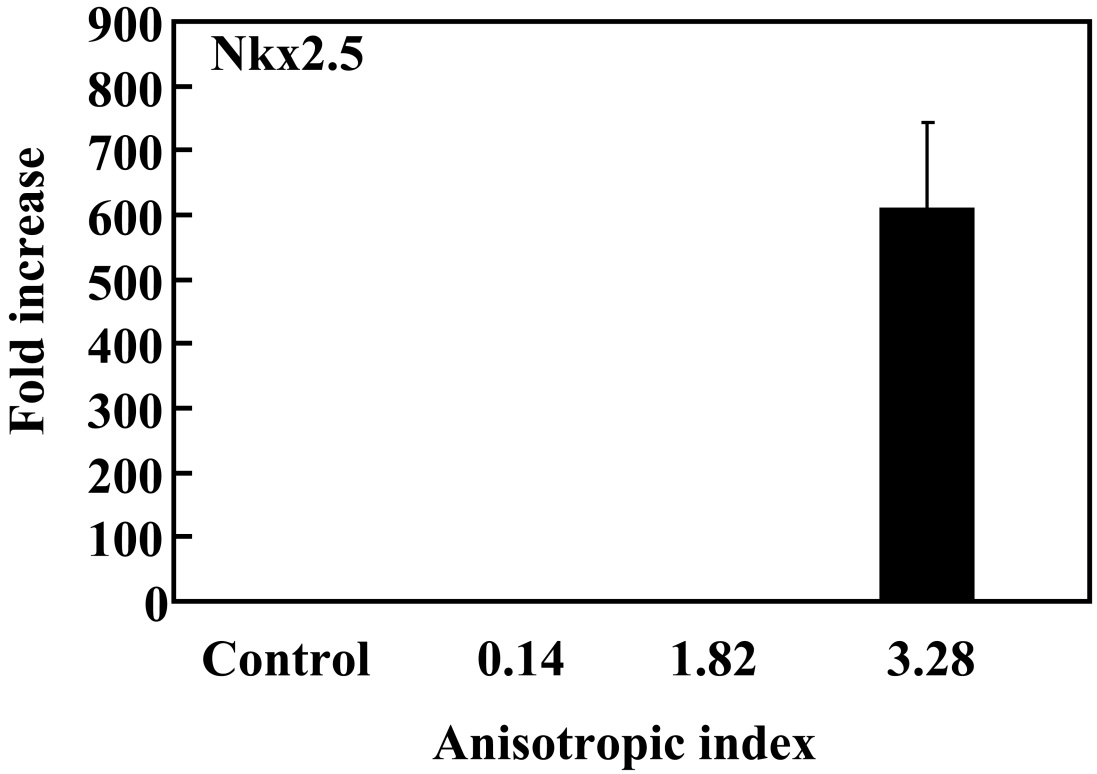

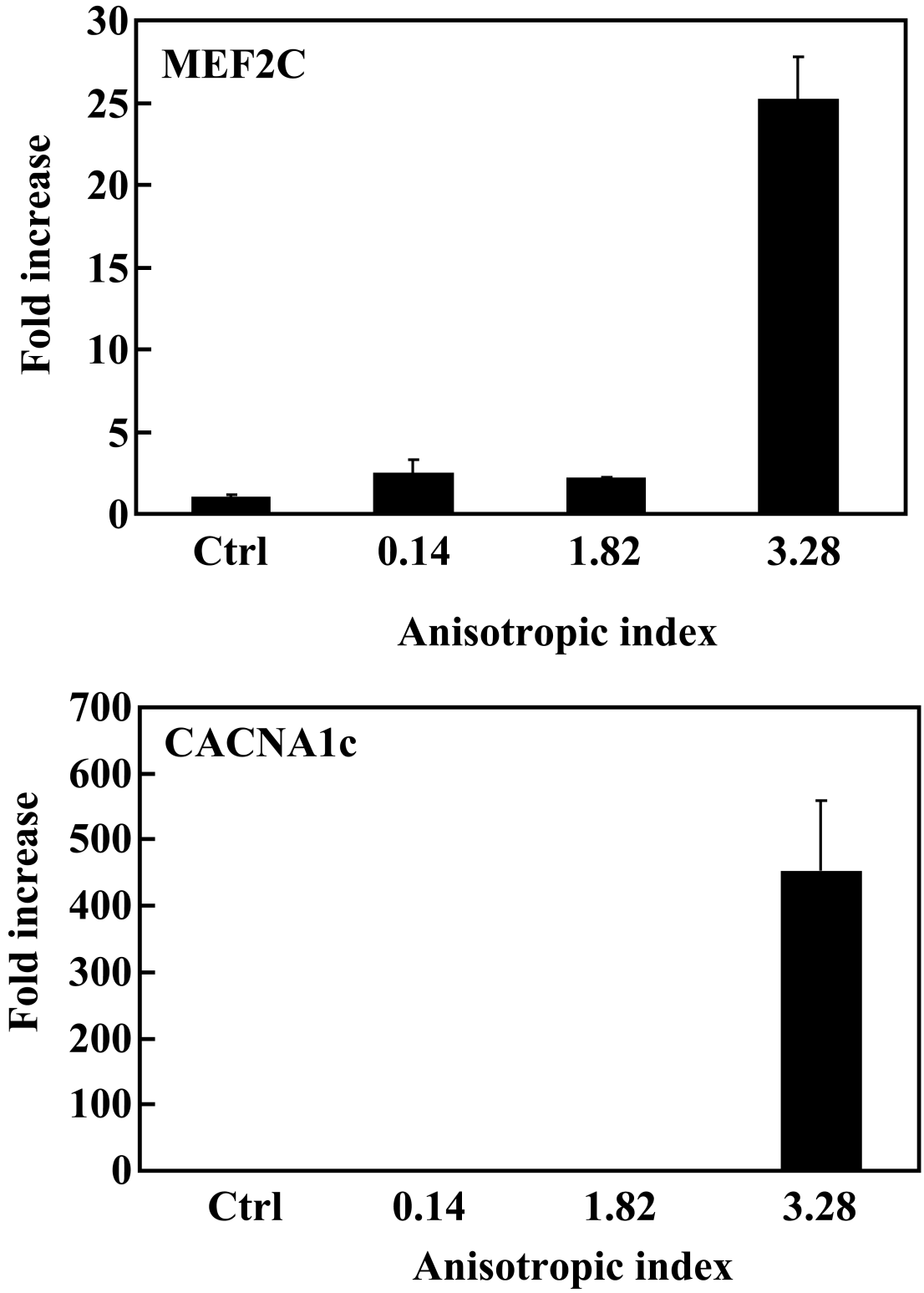

Figure 9.

Real-time RT-PCR analysis of cardiac specific genes GATA4, Nkx2.5 and MEF2C, and calcium channel CACNA1c. MSCs cultured on tissue culture plate were used as control (ctrl). The expression of these genes in control group was used for normalization.

Table 1

PCR primers

Gene	Prime sequences (Forward and Reverse)	Tm (°C)*
Collagen Type 1 (α1)	5′-CCGGAAACAGACAAGCAACCCAAA-3′ 3′-AAAGGAGCAGAAAGGGCAGCATTG-5′	73.2 71.8
Osteonectin	5′-TTCTGCCTGGAGACAAGGTGCTAA-3′ 3′-TCTGTTACTTCCCTTTGCCCACCT-5′	69.8 69.4
PPARγ2	5′-CTGTTTGCCAAGCTGCTCCAGAAA-3′ 3′-AAGAAGGGAAATGTTGGCAGTGGC-5′	72.1 71.6
Nkx2.5	5′-GGTGGAGCTGGAGAAGACAGA-3′ 3′-CGACGCCGAAGTTCACGAAGT-5′	65.7 67.8
GATA4	5′-AGCAGCTCCTTCAGGCAGT-3′ 3′-GCCCATGGCCAGACATC-5′	66.2 62.9
MEF2C	5′-GATCATCTTCAACAGCACC-3′ 3′-GTTCAATGCCTCCACGA-5′	59.5 60.5
CACNA1c	5′-CAGAAACTACAGGAGAAGAGG-3′ 3′-AAGAAGAGGATCAGGTTGGT-5′	59.5 60.5
(β-Actin	5′-AAGATCAAGATCATTGCTCCTC-3′ 3′-GGACTCATCGTACTCCTG-5′	61.2 59.5

* Tms were calculated by NIH PerlPrimer software.